ACS Combinatorial Science

Research Article

pubs.acs.org/acscombsci

Combinatorial Characterization of TiO_2 Chemical Vapor Deposition Utilizing Titanium Isopropoxide

Michael Reinke,*[,†,‡] Evgeniy Ponomarev,[‡,§] Yury Kuzminykh,[†,‡] and Patrik Hoffmann[†,‡]

[†]Laboratory for Advanced Materials Processing, Empa, Swiss Federal Laboratories for Materials Science and Technology, Feuerwerkerstrasse 39, CH-3602 Thun, Switzerland

[‡]Laboratory for Photonic Materials and Characterization, Ecole Polytechnique Fédérale de Lausanne, Station 17, CH-1015 Lausanne, Switzerland

ABSTRACT: The combinatorial characterization of the growth kinetics in chemical vapor deposition processes is challenging because precise information about the local precursor flow is usually difficult to access. In consequence, combinatorial chemical vapor deposition techniques are utilized more to study functional properties of thin films as a function of chemical composition, growth rate or crystallinity than to study the growth process itself. We present an experimental procedure which allows the combinatorial study of precursor surface kinetics during the film growth using high vacuum chemical vapor deposition. As consequence of the high vacuum environment, the precursor transport takes place in the molecular flow regime, which allows predicting and modifying precursor impinging rates on the substrate with comparatively little experimental effort. In this contribution, we study the surface kinetics of titanium dioxide formation using titanium tetraisopropoxide as precursor molecule over a large parameter range. We discuss precursor flux and temperature dependent morphology, crystallinity, growth rates, and precursor deposition efficiency. We conclude that the surface reaction of the adsorbed precursor molecules comprises a higher order reaction component with respect to precursor surface coverage.

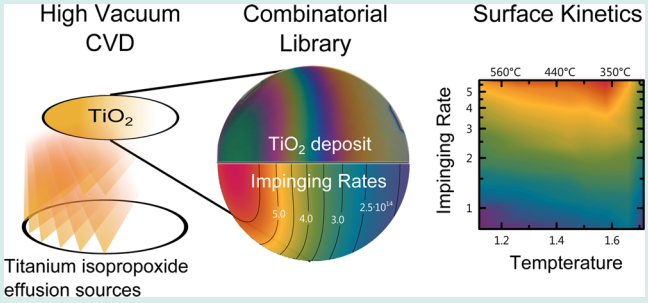

KEYWORDS: *combinatorial chemical vapor deposition, surface kinetics, surface reactions, titanium dioxide, titanium tetraisopropoxide, high vacuum chemical vapor deposition*

INTRODUCTION

Titanium dioxide is a highly versatile material that is not only widely used in all-day consumables such as paint, sunscreens or toothpaste, but represents also one of the most promising candidates for energy and environmental applications, because of its distinct photocatalytic properties.[1] Applications of titanium dioxide thin films reach from self-cleaning and self-sterilizing surfaces over water and air purification to heat transfer and heat dissipation and have been reviewed to great extent by Fujishima et al.[2]

Combinatorial deposition experiments allow the realization of a huge variety of compositions within a single experiment, a so-called "library".[3,4] Afterward, local measurements enable the extraction of specific properties as a function of composition, growth rate, substrate temperature, etc. In most of the cases physical vapor deposition techniques are employed for combinatorial deposition experiments, since the controlled realization of composition variations along a substrate is easier achieved than in classical chemical vapor deposition (CVD) processes.

A variety of reports have been published for the combinatorial survey of different TiO_2 systems by combinatorial atmospheric pressure CVD, for example, TiO_2/SnO_2,[5] TiO_2/W,[6] or TiO_2/VO_2.[7] The authors focus on the characterization of functional properties of the deposited thin films rather than on the growth process itself. To analyze the growth process, it is necessary to correlate the obtained growth rates and properties with the actual growth conditions, that is, with local distribution of precursor flow on the substrate. For low pressure CVD systems, a segmented precursor delivery system allows the performance of combinatorial experiments while keeping the precursor flow within the different segments controlled.[8,9] However, for this approach, relatively complex simulations are necessary to determine the actual flow conditions within each segment and correlate precursor flow and growth rates or functional properties.

In contrast, the design and calculation of precursor impinging rates in high vacuum chemical vapor deposition (HV-CVD) systems is possible using a comparatively simple analytical approach.[10] The high vacuum environment excludes gas phase reactions as the process is solely dependent on surface reactions of the adsorbed precursor molecules. HV-CVD therefore represents a useful tool for the combinatorial investigation of surface reactions during deposition processes. It has previously

Received: March 9, 2015
Revised: April 27, 2015
Published: June 2, 2015

DOI: 10.1021/acscombsci.5b00040
ACS Comb. Sci. 2015, 17, 413−420

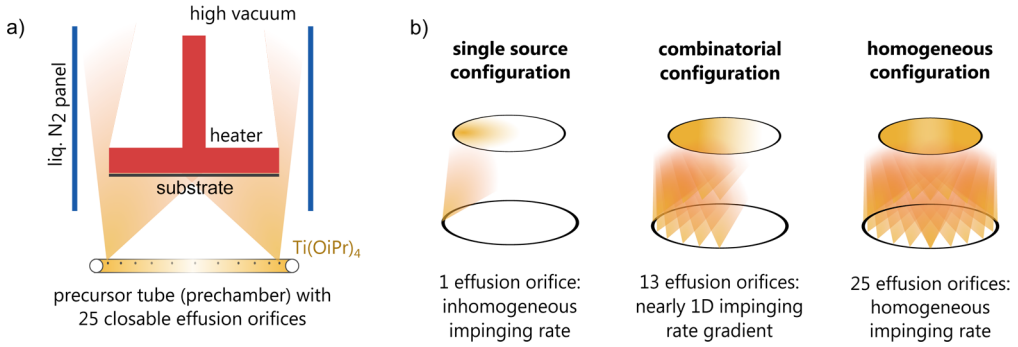

Figure 1. HV-CVD reactor consists of main reactor chamber containing substrate heater, holder, and liquid nitrogen panel and a separated precursor pipe ring with small individually closable orifices; depending on the configuration either homogeneous or gradient precursor impinging rates can be realized.

been used to optimize and analyze the deposition of $LiNbO_3$ thin films on sapphire.[11−14]

In this Research Article, we present in detail the experimental procedure for the combinatorial analysis of the deposition kinetics of titanium tetraisopropoxide ($Ti(OiPr)_4$) for the deposition of titanium dioxide utilizing high vacuum chemical vapor deposition (HV-CVD) at high temperatures (T > 300 °C). The deposition kinetics of $Ti(OiPr)_4$ is the subject of intense discussions in literature, mostly for the deposition in low pressure CVD systems. Here, the deposition reaction is highly dependent on the choice and amount of carrier gas.

Takahashi et al.[15] reported that the growth rate of titania is first order with respect to the gas phase concentration of titanium tetraisopropoxide, while the reaction order is 1.5 with respect to the nitrogen carrier gas flow rate. Assuming that the titanium mass flow is proportional to the carrier gas flow, this leads to a reaction order of 1.5 with respect of titanium tetraisorpopoxide concentration. These contradictory results were further analyzed by Siefering and Griffin,[16] who concluded that gas phase reactions determine the reaction order of the deposition process. In particular, they found that in carrier gas mixtures where the amount of nitrogen is small relative to the amount titanium isopropoxide, the reaction order becomes 2 with respect to the precursor molecule density. At larger nitrogen fractions, the reaction becomes first order. The authors rationalize this behavior by invoking a gas phase activation of precursor molecules and a subsequent surface reaction. The activation energy for this gas phase activation has been determined to be 40 kJ/mol in a hot-wall reactor.

As we are mainly interested in the surface kinetics, we cannot directly transfer these findings to our process, as it is very difficult to distinguish gas phase and surface reactions in conventional low-pressure CVD experiments. Nevertheless, these results are an important indicator that $Ti(OiPr)_4$ is able to self-catalyze the decomposition process and that higher order kinetics has to be taken into consideration when describing surface reactions.

Ideally, the experimental setup allows the discrimination between gas phase reactions of precursor molecules prior to their arrival at the substrate and actual surface reactions. This separation is easiest, when gas phase reactions can be neglected as it is the case in high vacuum systems. The surface kinetics of $Ti(OiPr)_4$ have been investigated by Taylor et. al,[17] who have performed HV-CVD experiments aiming to analyze the deposition rates as a function of temperature. The authors argue that in their experimental conditions, the surface reaction of $Ti(OiPr)_4$ is first order with respect to surface coverage, although the impinging rate was only varied over a small parameter range. Wu et al. have studied the reaction order as a function of precursor impinging rates by temperature-programmed reaction spectroscopy and concluded as well that the data are in agreement to a first-order reaction.[18]

We present here the analysis of high temperature (T > 300 °C) chemical vapor deposition of titanium dioxide films using combinatorial HV-CVD, varying the temperature between 310 and 620 °C and the precursor flux between 0.8×10^{14} cm^{-2} s^{-1} and 60×10^{14} cm^{-2} s^{-1}. The films were analyzed for mass thickness and chemical composition to derive the incorporated titanium atoms and quantify the number of successful precursor decomposition reactions. We will illustrate that the surface decomposition cannot be solely first order with respect to the precursor surface coverage and discuss the influence of deposition temperature and precursor impinging rate on the crystallinity of the formed films.

EXPERIMENTAL PROCEDURES

We use high-vacuum chemical vapor deposition (HV-CVD) for the combinatorial characterization of the deposition performance of titanium tetraisopropoxide at temperatures above 300 °C. In this section we briefly review the most important aspects of HV-CVD emphasizing its differences to conventional atmospheric or low pressure CVD and its ability to perform combinatorial experiments with comparatively little experimental effort. Subsequently, we describe the experimental conditions used in this study and how the samples were analyzed.

Combinatorial High-Vacuum Chemical Vapor Deposition. HV-CVD relies on the reaction of precursor molecules on the substrate surface. At high temperatures, adsorbed precursor molecules decompose pyrolitically to form the thin film. Figure 1a illustrates our HV-CVD reactor design. Precursors evaporate from a thermostated reservoir into a heated ring pipe system (prechamber), which is located inside the main reactor. In our case, the prechamber contains 25 individually closeable orifices which allow precursor molecules to effuse into the reaction chamber, where they can react on the substrate surface.

In HV-CVD, the pressure in the main reactor is kept at high vacuum (10^{-6} hPa) during the deposition. Hence, the mean free path of the molecules exceeds the length of their trajectory between effusion orifice and substrate and the precursor transport takes place in the molecular flow regime. Consequently and contrary to conventional CVD processes the precursor transport to the surface is **not limited** by gas

DOI: 10.1021/acscombsci.5b00040
ACS Comb. Sci. 2015, 17, 413−420

diffusion through the so-called boundary layer, but is only limited by the number of precursor molecules effusing into the reactor. Furthermore, gas phase interactions of precursor molecules in the reactor are minimized and the growth process of the film is determined only by surface chemistry and surface kinetics.

The flux (or impinging rate) of the precursor molecules on the substrate surface is dependent on their effusion rate through the orifices, which is primarily determined by the precursor partial pressure in the prechamber: the higher the pressure, the higher the effusion rate. The ballistic nature of precursor transport in the molecular flow regime allows predicting precursor impinging rate on the substrate solely by geometric considerations (number, size, form and position of the effusion sources and position of the substrate).[10,19] Inside the reactor a liquid nitrogen cooled panel traps nonreacted precursor molecules; this ensures the high vacuum conditions during the process by collecting volatile reaction byproducts and avoids the multiple impingement of nonreacted precursor molecules. As the use of high vacuum does not permit the use of carrier gas highly volatile nonagglomerating precursors are a prerequisite for HV-CVD.

Combinatorial experiments are characterized by the simultaneous realization of many experimental conditions within a single process, creating a so-called library. In terms of thin film CVD, it is therefore necessary to realize different precursor impinging rates on a single substrate during a single deposition. In HV-CVD, combinatorial conditions can be attained by arranging the effusion sources (orifices) of precursor molecules into specific geometric configurations. Figure 1b demonstrates three simple orifice configurations. In the standard configuration, that is, where all 25 orifices are opened, the system is designed to realize a homogeneous impinging rate over the whole 100 mm substrate. If only a single effusion source is opened, the precursor impinging rate varies over the substrate. In our experiments, we use the combinatorial configuration, where the substrate is exposed through 13 effusion sources. This realizes a close to linear impinging rate gradient along the substrate, which is very suitable for the efficient investigation of growth conditions and precursor kinetics.

Film Preparation. All combinatorial experiments were performed using a semiautomatized high vacuum chemical vapor reactor in the combinatorial configuration (compare Figure 1b).

We deposited TiO_2 films on naturally oxidized 100 mm silicon substrates at temperatures between 310 and 620 °C. The $Ti(OiPr)_4$ impinging rates varied between 8×10^{13} cm^{-2} s^{-1} and 6×10^{15} cm^{-2} s^{-1}. The $Ti(OiPr)_4$ precursor reservoir temperature varied in dependence of the desired impinging rate between 20 and 35 °C to deliver sufficient partial precursor pressure to the prechamber. The pressure inside of the ring system was kept constant by a feedback PID loop, consisting of a heated MKS Baratron pressure gauge and an automatically controlled needle valve. To ensure the molecular flow regime of the precursor inside the main reactor, the background pressure never exceeded 1×10^{-5} hPa during the process. The deposition time varied between 20 and 45 min depending on the growth rate of the thin films, which we measured in situ using reflectometry, a thin film optical interference detection technique.

Film Preparation. In the ex-situ analysis we focused on the analysis of the morphology and crystallinity as well as on the of the titanium incorporation rate (number of incorporated titanium atoms per unit time, that is the growth rate of the film) and the precursor deposition efficiency.

We analyzed the crystallographic phases of our deposits using X-ray diffraction (XRD). The measurements were performed in grazing incidence configuration ($\Theta = 0.5°$) using a copper k_α X-ray source; k_β radiation was filtered using a thin 0.125 mm nickel foil. We correlate different crystallographic phases with the surface morphology using top-view scanning electron micrographs.

The precursor deposition efficiency quantifies the probability that a precursor molecule which interacts with the substrate decomposes and contributes to the deposition process. It can be quantified by dividing the growth rate by the precursor impinging rate.

We determined the chemical composition by energy dispersive X-ray spectroscopy (EDX). The utilized quantitative analysis algorithm allows the deconvolution of the EDX spectra and differentiates signals originating from the substrate and the deposit (Oxford, Aztec LayerProbe). In this way we can quantify the chemical composition of the thin film and its mass thickness, that is, the weight of the thin film per unit area.[20] The combination of these two parameters enables us to calculate the number of incorporated titanium atoms per unit area N_{Ti}[atoms cm^{-2}]. We prefer to discuss the absolute number of incorporated titanium atoms rather than comparing film thicknesses, since this value is independent of the density and microstructure of the films. It is furthermore preferable when fitting kinetic models to experimental data, as the incorporation rate corresponds to the absolute number of precursor decomposition processes.

To consolidate the values taken by EDX analysis, we analyzed selected samples by alternative, complementary techniques: spectroscopic ellipsometry and Rutherford backscattering spectroscopy (RBS).

Spectral ellipsometry allows determination of the refractive index n of the obtained film which is directly correlated to the volume density of the titanium atoms ρ_{Ti} via the Lorentz–Lorenz law $\rho_{Ti}[cm^{-3}] = ((n^2 - 1)/(n^2 + 2))\cdot(3/4\pi\alpha_m)$.[21] We took 5.18×10^{-24} cm^3 as the value of the molecular polarizability α_m of TiO_2 for light of the wavelength 589 nm from literature.[22] After measuring the film thickness d of the films by cross-section scanning electron microscopy (SEM) we were able to derive the number of incorporated atoms per unit surface by $N_{Ti}[atoms\ cm^{-2}] = \rho_{Ti}\cdot d$.

Rutherford backscattering spectroscopy relies on the energy loss of incident high energetic ions during elastic collisions with the deposited material. The chemical composition of the deposit can be derived by measuring the energy ratio between the backscattered ions and the incident ions. Depth profiles and the absolute volume density ρ_{Ti} of the deposit can be evaluated if the energy loss while passing the material is taken into account.

RESULTS AND DISCUSSION

In this section, we describe the precursor impinging rate and temperature dependent properties of the deposited titania films. We begin this part by presenting titanium incorporation or growth rate, and evaluate the reliability of the obtained EDX results by comparing them with RBS and spectroscopic ellipsometry evaluation. Furthermore, we discuss the precursor deposition efficiency, which will lead to the important conclusion that the surface reaction of the adsorbed titanium isopropoxide molecule cannot be solely first order with respect

DOI: 10.1021/acscombsci.5b00040
ACS Comb. Sci. 2015, 17, 413–420

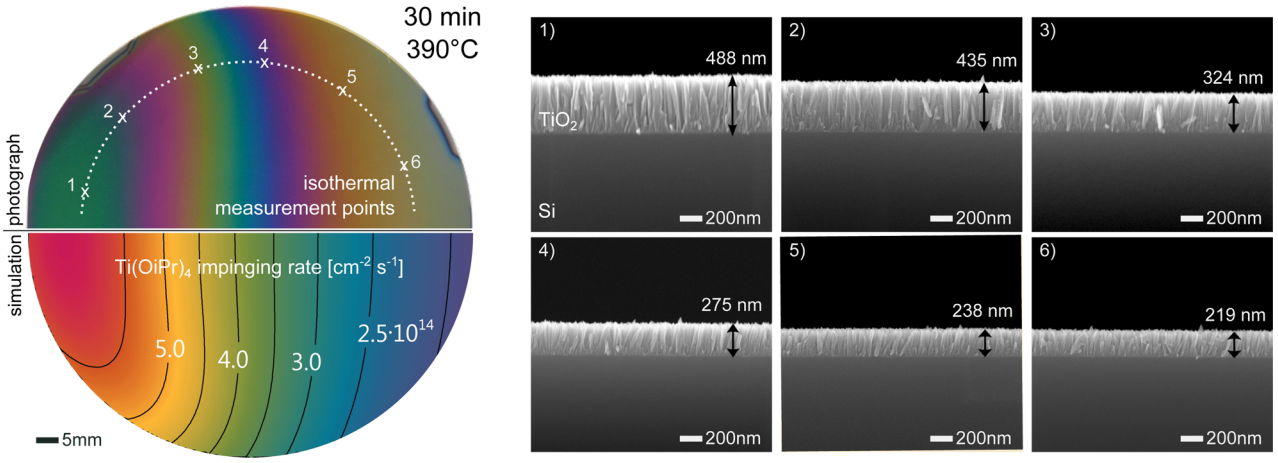

Figure 2. Photograph and simulation of a combinatorial experiment on a 100 mm silicon substrate, isothermal measurement points, which we used to minimize temperature differences between measurement points, are indicated in the upper part. Isoflux lines and precursor flux values [in cm^{-2} s^{-1}] are reported in the lower part. On the right we show scanning electron micrographs of the deposits cross sections and the averaged thickness measurements in nanometers to illustrate its variation over the substrate; the good agreement between simulation and deposition implies that the film was grown in the mass transport limited regime.

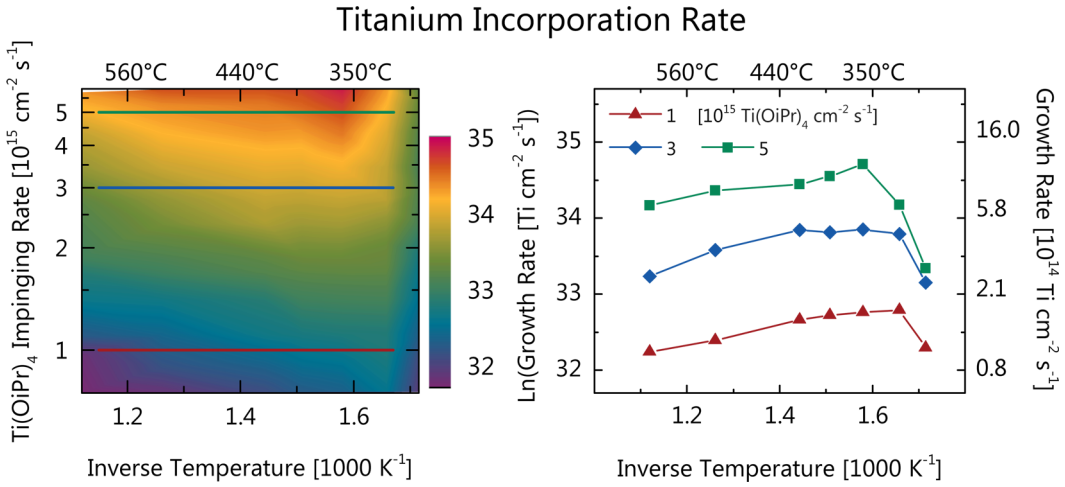

Figure 3. Titanium incorporation or growth rate is dependent on the substrate temperature and the precursor impinging rate. Depending on temperature and precursor flux, we identified different growth regimes, namely chemical reaction, mass flow and desorption controlled growth regime.

to the precursor surface coverage. In the final we illustrate film morphology and crystallinity of the titanium dioxide depositions.

$Ti(OiPr)_4$ Surface Kinetics. As previously mentioned, we aimed to efficiently screen many precursor impinging rates with a relatively small number of depositions. Accordingly we performed all deposition in the combinatorial configuration. To illustrate our methodology, we exemplary describe the evaluation of three measurement points on a single substrate. Figure 2 displays a photograph of one-half of a 100 mm substrate after a standard combinatorial titania deposition at 390 °C. In this experiment the gradient of precursor impinging rate leads to a film thickness variation along the substrate. The thickness gradient is visible as color-fringes on the photograph as result of the thin film interferences between the reflected light from the air/film and the reflected light from the film/substrate surface. The calculated impinging rates are displayed on the lower part of the figure. In this example, the precursor impinging rate ranges from 5.75×10^{15} cm^{-2} s^{-1} on the left to 2.0×10^{15} cm^{-2} s^{-1} on the right side. For the shown deposition, the color fringes resemble the precursor impinging rates meaning that the growth rate is proportional to the mass flow, which means that the deposition took place in the mass transport controlled regime.

To ensure isothermal growth conditions for all analyzed positions, we decided to characterize the films along an isothermal arc on the substrate, which is indicated also in Figure 2. By measuring the chemical composition and mass thickness only on positions along this arc of constant distance from the substrate center, we minimize the influence of possible temperature heterogeneities due to our cylindrical symmetric heater system.

For the three indicated points, 1, 3, and 6, on Figure 2 the precursor impinging rates were 5.5×10^{15}, 4.5×10^{15}, and 2.3×10^{15} cm^{-2} s^{-1}, respectively. We measured the thickness of the deposits to be 488, 324, and 219 nm by cross-section SEM, which are also shown. The resulting growth rates are 16.2, 10.8, and 7.3 nm min^{-1}. The corresponding micrographs confirm that the polycrystalline TiO_2 films exhibit a columnar growth behavior; for a detailed discussion of crystallinity and

DOI: 10.1021/acscombsci.5b00040
ACS Comb. Sci. 2015, 17, 413−420

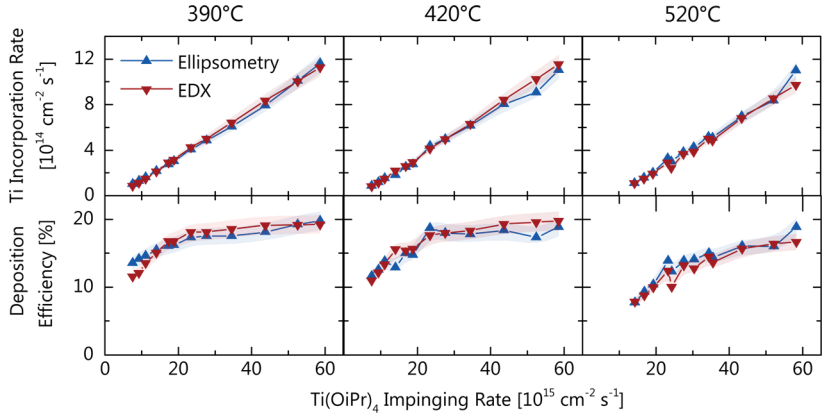

Figure 4. Titanium incorporation rate and precursor deposition efficiency for different temperature as a function of titanium impinging rate is depicted. Shown are the results of the EDX analysis and of the measurements by spectroscopic ellipsometry The increasing precursor efficiency indicates that the pyrolysis of $Ti(OiPr)_4$ cannot be solely first order with respect to $Ti(OiPr)_4$ surface coverage. For more details please refer to the text.

morphology we refer to the dedicated section. We characterized the chemical composition and the mass thickness by quantitative EDX measurements. Within experimental uncertainties, the deposited films were stoichiometric; the carbon contamination was below the detection limit. The mass thicknesses of the films are 138, 86, and 51 $\mu g\ cm^{-2}$, respectively. With the chemical composition of the films the titanium atom incorporation rate was derived to be 5.8×10^{14}, 3.6×10^{14}, and $2.1 \times 10^{14}\ cm^{-2}\ s^{-1}$.

Following the same methodology, we have analyzed in total 84 data points, corresponding to 14 combinatorial deposition experiments with six data points per substrate. Figure 3 shows the growth rate or titanium incorporation rate as a function of precursor impinging rate and temperature.

The deposition rate in an HV-CVD process is determined by the interplay between precursor impinging, desorption and decomposition reaction rate of the participating precursors. Therefore, the growth rate can be separated into different growth regimes with respect to the substrate temperature and precursor flux: (a) the chemical reaction controlled regime, where the rate of impinging precursors exceeds the rate of chemical reaction on the surface, but the film growth cannot follow the latter one; (b) the mass flow controlled regime, where the opposite is the case; and (c) the desorption controlled regime, where the rate of precursor desorption increases more rapid than the decomposition rate of the precursor at higher substrate temperatures and hence the growth rate drops. Compared to conventional CVD, precursors do not interact multiple times with the surface but are trapped by a liquid nitrogen panel after desorption to keep the reactor in a high vacuum environment. Therefore, the precursor desorption ultimately limits the deposition efficiency. Within our parameter range, the highest measured precursor deposition efficiency is 23%.

Generally, we observe in our experiments that the incorporation rate increases with increasing precursor impinging rate and that the growth rate is less dependent on the substrate temperature for films deposited at low precursor fluxes. At low temperatures below 350 °C, the growth rate increases, when increasing the substrate temperature. This indicates that the growth is limited by the chemical reaction rate of the adsorbed precursor molecules and that in this conditions, the film growth takes place in the chemical reaction limited regime. For higher substrate temperatures, in the range between 350 and 440 °C the growth rate is nearly independent of the substrate temperature; the film growth is mass flow limited. In particular for an impinging rate of $3 \times 10^{15}\ cm^{-2}\ s^{-1}$, the constant growth rate is visible. At higher temperatures, the growth rates decrease due to the higher desorption rate of precursor molecules prior to decomposition and the growth becomes desorption limited.

Figure 4 depicts the growth rate and precursor deposition efficiency for three different temperatures: 390 °C, 420 and 520 °C. In all cases the incorporation rate increases with increasing precursor impinging rate. At the deposition temperatures of 420 °C the slope of the incorporation rate is purely linear to the $Ti(OiPr)_4$ impinging rate, indicating that the deposition rate was purely mass flow controlled. This holds also true for the depositions at 520 °C substrate temperature; the absolute growth rates, however, are smaller compared to the deposition rates at 420 °C. At 520 °C the precursor desorption prior to deposition already limits the growth rate.

The same figure depicts also the precursor deposition efficiency of $Ti(OiPr)_4$ at different temperatures, which is the ratio of incorporation rate and precursor impinging rate. At low impinging rates (below $2 \times 10^{15}\ cm^{-2}\ s^{-1}$ at 390 °C for instance) the deposition efficiency increases with increasing impinging rate, the efficiency of precursor decomposition first increases with increasing precursor flux. This is a surprising finding and as we will discuss later, this behavior indicates that it is necessary to consider also higher-order reactions with respect to the surface coverage to explain the surface decomposition of adsorbed precursor molecules.

Titanium Isopropoxide Reaction Order. In the introduction, we have reviewed the available literature dealing with the deposition kinetics of $Ti(OiPr)_4$ in CVD and HV-CVD processes. In the first case, the reaction order of the deposition process with respect to the $Ti(OiPr)_4$ concentration depends mainly on the type and composition of the carrier gas. In the latter case, where the growth rate is determined by surface kinetics, it is believed that the surface reaction of the adsorbed precursor molecule is first order with respect to the $Ti(OiPr)_4$ surface coverage.

In our experiments, however, we need to consider also a second-order contribution to explain the kinetics of the process. In fact, the observed increase of precursor deposition efficiency

DOI: 10.1021/acscombsci.5b00040
ACS Comb. Sci. 2015, 17, 413−420

with increasing precursor flux cannot be rationalized assuming solely a first order reaction of $Ti(OiPr)_4$ with respect to the precursor's surface coverage. Assuming first-order kinetics, the probability that a chemisorbed molecule decomposes (or desorbs) is independent from its surrounding and occupation density. The overall deposition efficiency would then only be determined by the steady state surface coverage of the substrate. At high surface coverages, a part of the impinging precursor molecules cannot adsorb on the surface. Hence, we would expect a decrease of deposition efficiency with increasing precursor impinging rate. In contrary we have observed an increase of deposition efficiency with increasing precursor impinging rate, for example, with increasing surface coverage.

Therefore, we conclude, that the nature of at least one of the reactions paths for the decomposition of adsorbed titanium isopropoxide is of higher-order than one with respect to the adsorbed precursor surface coverage.

Consolidation of EDX Analysis. We mostly analyze our samples by EDX. This technique offers an efficient way to characterize large amounts of samples in relatively short time. In order to increase the reliability of the obtained values, some samples have been additionally evaluated by spectroscopic ellipsometry as has been described above. We have found that depending on growth conditions, the refractive index of the obtained films vary between 1.592 and 2.077 at a wavelength of 589 nm. The refractive index of the material is related to the volume density by the Lorentz−Lorenz law. Additionally we measured the thickness by cross-section SEM to obtain the incorporation rate and deposition efficiency. The obtained values for the samples grown at 390, 420, and 520 °C substrate temperature are depicted in the already discussed Figure 4 along with the values that we derived using EDX analysis. Within the measurement uncertainties, both analysis lead to the same results.

Additionally, we have characterized four samples concerning their chemical composition and mass density by Rutherford backscattering. These measurements confirm the stoichiometric nature of the titanium dioxide films. Table 2 compares the obtained incorporation rates for different temperatures and impinging rates. Assuming that the RBS measurements are more precise, the relative error of the quantitative EDX measurements does not exceed 10.2%.

In conclusion, we confirmed the EDX results by two independent measurement techniques, supporting the feasibility of EDX as rapid analyzing technique for combinatorial HV-CVD experiments.

Morphology and Crystallinity. Figure 5 shows scanning electron micrographs of titanium dioxide films grown at different temperatures and precursor impinging rates. All images indicate the crystalline nature of the deposited films. A direct comparison of the micrographs is difficult because generally different deposition durations and conditions lead to different film thicknesses. However, as also visible in Figure 3, the growth rates at 310 and 620 °C are almost identical for the low flux used (1.5×10^{15} cm^{-2} s^{-1}). Therefore, we can compare their appearance and grain size directly and find that with increasing substrate temperature the grain size of the deposit increases—this is expected as the additional thermal energy enhances the surface diffusion length. More general, the morphology of the films changes at higher temperature.

The difference in morphology is also reflected in the crystallinity of the obtained deposits as shown in the XRD results in Figure 6. For depositions carried at 310 °C substrate temperature the crystalline phase of the grown titanium dioxide film is purely anatase at a precursor impinging rate of 1.5×10^{15} cm^{-2} s^{-1}. For higher deposition temperatures, we identify a mixture of anatase and rutile phases. At 620 °C a pure rutile phase is ultimately formed for this impinging rate. The gradual transition between anatase and rutile corresponds well previously reported results, where an onset of rutile formation was reported at 400 °C.[23] As can be seen also in Figure 6, at 620 °C substrate temperature an anatase phase forms, if the precursor impinging rate is increased. We believe that this behavior is connected to a decreased surface mobility at higher fluxes due to enhanced surface occupation.

The fraction of anatase to rutile formation can be calculated for powders using the following relation $(1 + 1.265(I_R/I_A))^{-1}$ where I_R denotes the peak intensity of the rutile (110) reflection and I_A the peak intensity of the anatase (101) reflection.[24] If we assume comparable crystallite sizes for all films and random orientation of the phases, we can use the equation to obtain an indication concerning the anatase to rutile ration in our deposits. As can be seen in Figure 6, the rutile to anatase ratio reaches about 50% and a substrate temperature of 520 °C for an impinging rate of 1.5×10^{15} cm^{-2} s^{-1}. Furthermore, we see, that at high substrate temperatures (620 °C) and the rutile to anatase ratio increases from 1:0 for low impinging rates (1.5×10^{15} cm^{-2} s^{-1}) to 0.9:0.1 for high fluxes (4.5×10^{15} cm^{-2} s^{-1}).

Table 1. Comparison between Quantitative EDX and RBS Analysis of Four Samples Grown by HV-CVD[a]

temperature [°C]	$Ti(OiPr)_4$ impinging rate [10^{15} cm^{-2} s^{-1}]	incorporation rate [10^{15} cm^{-2} s^{-1}]		deposition efficiency [%]		
		RBS	EDX	RBS	EDX	Δ [%]
360	2.34	0.23	0.23	9.7	9.7	0.4
360	5.85	0.30	0.27	5.2	4.6	−10
390	0.75	0.15	0.16	19.9	21.1	6.0
390	1.88	0.45	0.46	23.9	24.6	2.9

[a]The titanium incorporation rate and deposition efficiency was derived and compared by independent techniques to judge the precision of EDX analysis.

CONCLUSIONS

We have shown an experimental procedure to rapidly investigate the surface kinetics of titanium dioxide deposition using titanium tetra isopropoxide ($Ti(OiPr)_4$) in chemical vapor deposition process over a large precursor impinging rate range at substrate temperatures between 310 and 610 °C by combinatorial high vacuum chemical vapor deposition (HV-CVD). In the high vacuum environment, gas phase interactions of the precursor molecules are suppressed and the reaction is entirely driven by surface reactions. Our samples were analyzed by scanning electron microscopy (SEM), energy dispersive X-ray analysis (EDX) and X-ray diffraction (XRD). Selected analyses were double checked either by spectroscopic ellipsometry or Rutherford-backscattering (RBS).

Depending on substrate temperature and precursor impinging rate anatase, rutile or a mixture of the two phases were formed during the deposition process. We have shown that only at sufficiently low precursor impinging rate the grown

DOI: 10.1021/acscombsci.5b00040
ACS Comb. Sci. 2015, 17, 413−420

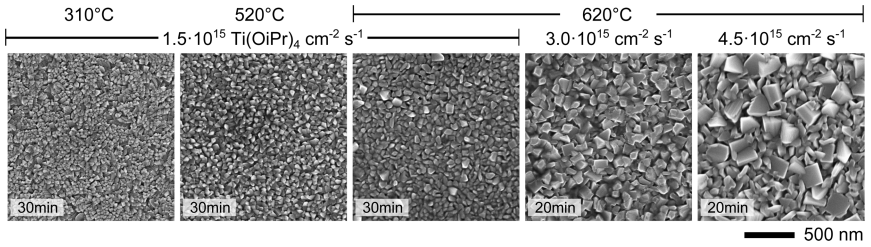

Figure 5. Top-view scanning electron micrographs of TiO_2 films formed under different conditions. The grain morphology changes as a function of precursor impinging rate as visible in the first four micrographs, were comparable film thickness were investigated. With increasing film thickness, the grain size grows, as visible in the fifth micrograph, where the film thickness is double compared to the other cases.

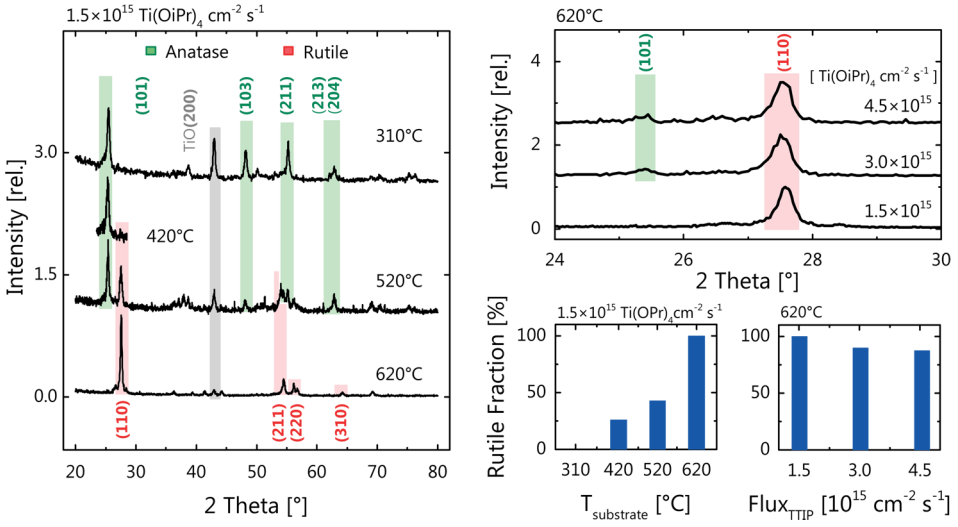

Figure 6. XRD analysis of the deposited TiO_2 films, while low temperature depositions lead to the formation of an anatase TiO_2 phase, high deposition temperatures favor the formation of the rutile phase. At 620 °C the ratio between anatase and rutile formation is dependent on the precursor impinging rate. At low temperatures a TiO (200) peak is visible, which's intensity diminishes at elevated substrate temperatures.

films are pure rutile at 620 °C and that the anatase traces starts to form when increasing the precursor flux.

Within the experiments performed for this study, we have identified different growth regimes for the deposition of TiO_2 at elevated temperatures, for example, a chemical reaction controlled regime below 330 °C and $Ti(OiPr)_4$ impinging rates below 5×10^{15} cm^{-1} s^{-2} and a mass transport controlled regime at higher temperatures. Throughout our experiments, desorption of adsorbed precursors limited the efficiency of the deposition process; hence the precursor deposition efficiency never exceeded 23%. Furthermore, we observed an increase of deposition efficiency with increasing flux in the mass transport controlled regime. As a simple first order reaction pathway is not sufficient to explain the increasing deposition efficiency with increasing precursor impinging rate, we conclude that the surface reaction also comprises a higher order component with respect to $Ti(OiPr)_4$ surface coverage.

We believe that combinatorial HV-CVD represents a versatile tool for the rapid characterization of the surface kinetics. Contrary to combinatorial atmospheric pressure CVD, it focuses on the efficient characterization of the growth process itself rather than on functional properties of the obtained film. Compared to combinatorial CVD, it offers precise control and predictability of precursor impinging rates and therefore enables combinatorial experiments with less experimental effort.

AUTHOR INFORMATION

Corresponding Author

*E-mail: michael.reinke@empa.ch. Phone: +41 58 765 62 22.

Present Address

§E.P.: Département de Physique de la Matiére Condensée (DPMC) and Group of Applied Physics (GAP), University of Geneva, 24 Quai Ernest-Ansermet, CH-1211 Genève, Switzerland.

Author Contributions

The manuscript was written through contributions of all authors. All authors have given approval to the final version of the manuscript.

Notes

The authors declare no competing financial interest.

ACKNOWLEDGMENTS

The authors express their gratitude to Max Döbeli, ETHZ for performing RBS measurements and analysis. Furthermore, we thank Saeed Mohammadi-Siyani for XRD characterization of the presented samples. We gratefully acknowledge the partial financial support of the Swiss National Science Foundation under Contract 200021_13504.

ABBREVIATIONS

CVD, chemical vapor deposition; HV-CVD, high vacuum CVD; ALD, atomic layer deposition; $Ti(OiPr)_4$, titanium tetraisopropoxide; SEM, scanning electron microscope; EDX,

DOI: 10.1021/acscombsci.5b00040
ACS Comb. Sci. 2015, 17, 413−420

energy dispersive X-ray analysis; RBS, Rutherford-backscattering

REFERENCES

(1) Chen, X.; Mao, S. S. Titanium dioxide nanomaterials: Synthesis, properties, modifications, and applications. *Chem. Rev. (Washington, DC, U. S.)* **2007**, *107* (7), 2891−2959.

(2) Fujishima, A.; Zhang, X. T.; Tryk, D. A. TiO_2 photocatalysis and related surface phenomena. *Surf. Sci. Rep.* **2008**, *63* (12), 515−582.

(3) Green, M. L.; Takeuchi, I.; Hattrick-Simpers, J. R., Applications of high throughput (combinatorial) methodologies to electronic, magnetic, optical, and energy-related materials. *J. Appl. Phys.* **2013**, *113* (23).

(4) Barber, Z. H.; Blamire, M. G. High throughput thin film materials science. *Mater. Sci. Technol.* **2008**, *24* (7), 757−770.

(5) Sathasivam, S.; Kafizas, A.; Ponja, S.; Chadwick, N.; Bhachu, D. S.; Bawaked, S. M.; Obaid, A. Y.; Al-Thabaiti, S.; Basahel, S. N.; Carmalt, C. J.; Parkin, I. P. Combinatorial atmospheric pressure CVD of a composite TiO_2/SnO_2 thin film. *Chem. Vap. Deposition* **2014**, *20* (1−3), 69−79.

(6) Kafizas, A.; Parkin, I. P. Combinatorial atmospheric pressure chemical vapor deposition (cAPCVD): A route to functional property optimization. *J. Am. Chem. Soc.* **2011**, *133* (50), 20458−20467.

(7) Wilkinson, M.; Kafizas, A.; Bawaked, S. M.; Obaid, A. Y.; Al-Thabaiti, S. A.; Basahel, S. N.; Carmalt, C. J.; Parkin, I. P. Combinatorial atmospheric pressure chemical vapor deposition of graded TiO_2−VO_2 mixed-phase composites and their dual functional property as self-cleaning and photochromic window coatings. *ACS Comb. Sci.* **2013**, *15* (6), 309−319.

(8) Choo, J. O.; Adomaitis, R. A.; Henn-Lecordier, L.; Cai, Y.; Rubloff, G. W. Development of a spatially controllable chemical vapor deposition reactor with combinatorial processing capabilities. *Rev. Sci. Instrum.* **2005**, *76* (6), 062217.

(9) Cai, Y.; Henn-Lecordier, L.; Rubloff, G. W.; Sreenivasan, R.; Choo, J.-O.; Adomaitis, R. A. Multiplexed mass spectrometry for real-time sensing in a spatially programmable chemical vapor deposition reactor. *J. Vac. Sci. Technol. B* **2007**, *25* (4), 1288−1297.

(10) Reinke, M.; Kuzminykh, Y.; Hoffmann, P. Limitations of patterning thin films by shadow mask high vacuum chemical vapor deposition. *Thin Solid Films* **2014**, *563* (0), 56−61.

(11) Dabirian, A. Combinatorial high-vacuum chemical vapor deposition of lithium niobate thin films. Thesis, École Polytechnique Fédérale de Lausanne, Lausanne, Switzerland, 2010; Thesis 4733.

(12) Dabirian, A.; Kuzminykh, Y.; Afra, B.; Harada, S.; Wagner, E.; Sandu, C. S.; Benvenuti, G.; Rushworth, S.; Muralt, P.; Hoffmann, P. Combinatorial discovery and optimization of amorphous HfO_2−Nb_2O_5 Mixture with Improved Transparency. *Electrochem. Solid-State Lett.* **2010**, *13* (7), G60−G63.

(13) Dabirian, A.; Kuzminykh, Y.; Sandu, S. C.; Harada, S.; Wagner, E.; Brodard, P.; Benvenuti, G.; Rushworth, S.; Muralt, P.; Hoffmann, P. Combinatorial High-Vacuum Chemical Vapor Deposition of Textured Hafnium-Doped Lithium Niobate Thin Films on Sapphire. *Cryst. Growth Des.* **2011**, *11* (1), 203−209.

(14) Dabirian, A.; Kuzminykh, Y.; Wagner, E.; Benvenuti, G.; Rushworth, S. A.; Hoffmann, P. Chemical Vapor Deposition Kinetics and Localized Growth Regimes in Combinatorial Experiments. *ChemPhysChem* **2011**, *12* (18), 3524−3528.

(15) Takahashi, Y.; Suzuki, H.; Nasu, M. Rutile growth at the surface of TiO_2 films deposited by vapour-phase decomposition of isopropyl titanate. *J. Chem. Soc., Faraday Trans. 1* **1985**, *81* (12), 3117−3125.

(16) Siefering, K. L.; Griffin, G. L. Growth kinetics of CVD TiO_2: Influence of carrier gas. *J. Electrochem. Soc.* **1990**, *137* (4), 1206−1208.

(17) Taylor, C. J.; Gilmer, D. C.; Colombo, D. G.; Wilk, G. D.; Campbell, S. A.; Roberts, J.; Gladfelter, W. L. Does chemistry really matter in the chemical vapor deposition of titanium dioxide? Precursor and kinetic effects on the microstructure of polycrystalline films. *J. Am. Chem. Soc.* **1999**, *121* (22), 5220−5229.

(18) Wu, Y.-M.; Bradley, D. C.; Nix, R. M. Studies of titanium dioxide film growth from titanium tetraisopropoxide. *Appl. Surf. Sci.* **1993**, *64* (1), 21−28.

(19) Benvenuti, G. Chemical beam deposition of titanium dioxide thin films. Thesis, École Polytechnique Fédérale de Lausanne, Lausanne, Switzerland, 2003; Thesis 2744.

(20) Reinke, M.; Kuzminykh, Y.; Malandrino, G.; Hoffmann, P. Precursor adsorption efficiency of titanium tetra isopropoxide in the presence of a barium β-diketonate precursor. *Surf. Coat. Technol.* **2013**, *230* (0), 297−304.

(21) Kittel, C.; McEuen, P.; McEuen, P. *Introduction to Solid State Physics*; Wiley: New York, 1976; Vol. *8*.

(22) Khawaja, E.; Bouamrane, F.; Al-Adel, F.; Hallak, A.; Daous, M.; Salim, M. Study of the Lorentz−Lorenz law and the energy loss of 4 He ions in titanium oxide films. *Thin Solid Films* **1994**, *240* (1), 121−130.

(23) Byun, C.; Jang, J. W.; Kim, I. T.; Hong, K. S.; Lee, B. W. Anatase-to-rutile transition of titania thin films prepared by MOCVD. *Mater. Res. Bull.* **1997**, *32* (4), 431−440.

(24) Spurr, R. A.; Myers, H. Quantitative analysis of anatase−rutile mixtures with an X-ray diffractometer. *Anal. Chem.* **1957**, *29* (5), 760−762.

DOI: 10.1021/acscombsci.5b00040
ACS Comb. Sci. 2015, 17, 413−420